Supporting Information

Surface Plasmon Resonance Induced High Optical Performance for VO_2@SiO_2 Nanorods-based Thermochromic Window

Formation mechanism of VO_2 precursor nanorods

The formation mechanism of VO_2 precursor nanorods can be explained by considering six-coordinated zero-charge monomers $[VO(OH)_2(OH_2)_3]$ in equilibrium with the decavanadate. As soon as the monomers appear in solution, these entities could be condensed by olation and oxolation; olation reactions, in which labile water molecules are apt to break away, are kinetically faster than oxolation reactions.The formation of chains is the result of the structure of the precursors; short V=O bonds prevent condensation along their axis since V=O bonds destroy the nucleophilic character of such ligands, leaving them only slightly basic and not prone to protonation. The zero-charge monomers $[VO(OH)_2(OH_2)_3]$ can be condensed along the directions of V-OH and V-OH_2, where V-OH_2 is more liable for condensation.[1-3]The methods of decondensation can be summarized in Scheme 1, and Scheme 2 gives a possible formation mechanism of VO_2nanorods from $[VO(OH)_2(OH_2)_3]$.

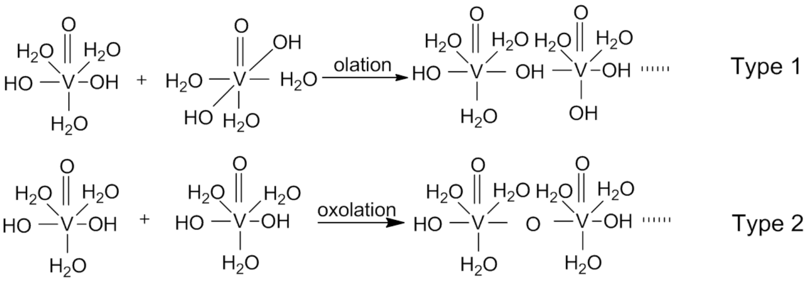

Scheme S1 the styles of olation and oxolation

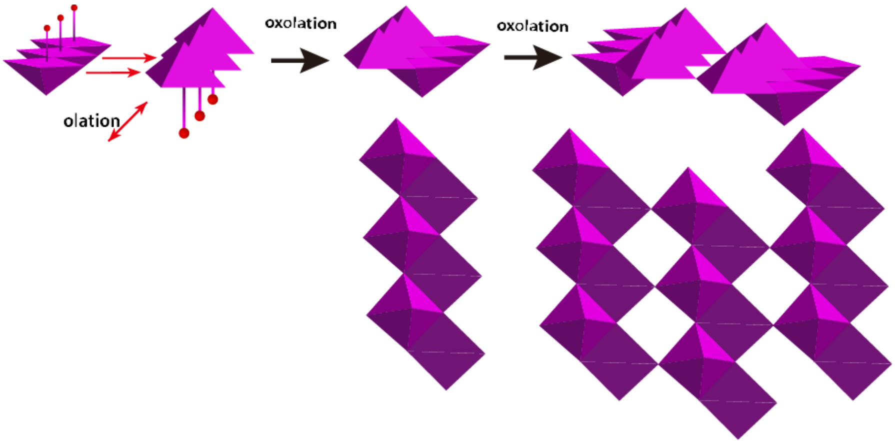

Scheme S2 Possible formation mechanism of VO2 nanorods from [VO(OH)2(OH2)3]

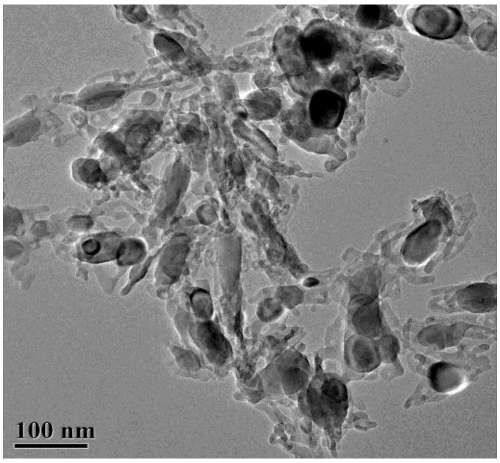

Figure S1 A TEM image of Sample A2 after heat treatment at 800^{o}C for 20 min

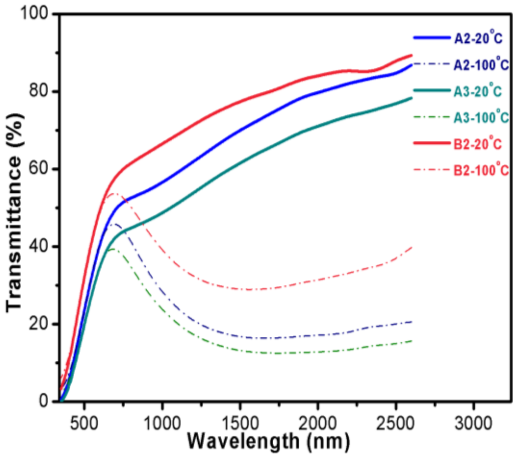

Figure S2 Optical transmittance spectra for Sample A2, B2, C2. Extending the heat treatment time, the phenomenon of SPR disappears for the aggregation and growth of VO$_2$ nanoparticles

Table S1 Optical properties of flexible foils for Sample A2, A3, B2

Sample	**T_{lum} (%)**		**T_{Sol} (%)**		**$\triangle T_{Sol}$(%)**
	T<Tc	**T>Tc**	**T>Tc**	**T<Tc**	
A2	36.81	34.68	30.05	47.72	16.16
A3	31.49	29.63	25.34	41.39	15.05
B2	45.54	42.79	39.26	56.12	15.85

Simulation

In order to investigate the variation of λ_{SPR} with different content of SiO_2, we can firstly suppose a simple model: assuming that VO_2nanorods are dispersed in the continuous SiO_2 host, which is reasonable because VO_2 is totally coated by SiO_2. The fact can be similar with Lopez's report.[4] When environmental temperature is higher than Mott phase transition (Tc), VO_2 nanorods are being metallic state, which can be regarded as metal nanorods. For predicting the variation of λ_{SPR} quantitatively, the Maxwell-Garnett (MG) theory can be introduced due to its simplicity and validity for separated-grain structure in which particles of one component are dispersed in a continuous host. Its validity can be further improved if geometrical effects of nonspherical particles are taken into consideration. The effective dielectric constant of the VO_2(R)-separated film in this case is expressed as:

$$\frac{\varepsilon_s(\omega)-\varepsilon_{av}(\omega)}{L_m\varepsilon_s(\omega)+(1-L_m)\varepsilon_{av}(\omega)}=q\frac{\varepsilon_m(\omega)-\varepsilon_{av}(\omega)}{L_m\varepsilon_m(\omega)+(1-L_m)\varepsilon_{av}(\omega)} \qquad (1)$$

Where

q is the particle filling factor of metallic islands ($0< q <1$),

L_m is the depolarization factor corresponding to the shape of the metal particles,

$\varepsilon_{av}(\omega)$ is the interisland dielectric constant given by $(n_s^2+1)/2$, an average of the contribution from the substrate and air, for VO_2 nanorods was totally coated by SiO_2, so $\varepsilon_{av}(\omega)=n^2_{SiO_2}$,

$\varepsilon_m(\omega)$ is the complex dielectric constant of the metallic particles,

$\varepsilon_m(\omega)=\varepsilon_{m1}(\omega)+i\varepsilon_{m2}(\omega)$. For a real metal, $\varepsilon_{m1}(\omega)$, $\varepsilon_{m2}(\omega)$ can be described with the Drude model, that is,

$$\varepsilon_{m1}(\omega)=\varepsilon_\infty-\frac{\omega_p^{\ 2}}{\omega^2+1/\tau^2} \quad (2) \quad \text{and} \quad \varepsilon_{m2}(\omega)=\frac{\omega_p^{\ 2}/\tau}{\omega(\omega^2+1/\tau^2)} \quad (3)$$

Where ω_p and τ are the free-electron plasma frequency and the collision time respectively. ε_∞ is the high frequency dielectric constant due to interband transitions of electrons.

The SPR frequency is defined as the frequency for which $\mathrm{Re}[\varepsilon_s(\omega_{SPR})]=0$.

Substituting (2) and (3) into (1) and solving equation for this condition, then

$$\omega_{SPR}^{\ 2}=\omega_p^{\ 2}\frac{(1-q)L_m}{\varepsilon_{av}-(\varepsilon_{av}-\varepsilon_\infty)(1-q)L_m}-\frac{1}{\tau^2} \quad (4)$$

It was demonstrated that τ has very limited effects on ω_{SPR} and can be ingored in (4).[26,27] Thus, the SPR, $\lambda_{SPR}(\equiv 2\pi c/\omega_{SPR})$, is given by

$$\lambda_{SPR}=\lambda_p\left[\frac{\varepsilon_{av}}{(1-q)L_m}-\varepsilon_{av}+\varepsilon_\infty\right]^{\frac{1}{2}} \quad (5)$$

Where $\lambda_p=2\pi c/\omega_p$, the metal's bulk plasma wavelength. To obtain the value of L_m and simplify the computation, we can consider VO_2 nanorods as long ellipsoids. Then three depolarization factor along the three axis can be met following equation: $L_x+L_y+L_z=1$(for sphere, $L_x=L_y=L_z=1/3$)

We assume that $x>y, y=z, x/y=m, m>1$ then $L_y=L_z=(1-L_x)/2$;

According to the equation[5]

$$L_x=\frac{1}{1-m^2}+\frac{m}{\sqrt{(m^2-1)^3}}\ln(m+\sqrt{m^2-1}) \quad (6)$$

$$L_y=L_z=\frac{1}{2}\left[\frac{m^2}{m^2-1}-\frac{m}{\sqrt{(m^2-1)^3}}\ln(m+\sqrt{m^2-1})\right] \quad (7)$$

When the incident light irradiates on the surface of film and the light is perpendicular to the long axis of nanorods , so the depolarization factor $L_m=L_y=L_z$. Combined the equation (7) with (5), other parameters can be obtained from Hans W. Verleur's paper.[6] The simulating result was shown in Figure 4C.

Experimental details

1 Preparation of $VOCl_2$ solution

The $VOCl_2$ solution was prepared by reduction of commercial vanadium pentoxide (V_2O_5, 99%, Sinopharm Chemical Reagent) with hydrazine monohydrate($N_2H_4 \cdot H_2O$, 99%, Sigma) in the presence of hydrochloric acid (HCl, AP, Sinopharm Chemical Reagent). Typically, 100.0 mL 1M HCl solution and 10.0 g V_2O_5 were mixed under magnetic stirring at 60°C, 2.0 mL hydrazine monohydrate was slowly dropped into the above mixed solution. The reaction was kept for 2h until the solution was turned into transparent blue, indicating that the V^{5+} has been reduced to V^{4+}. The final solution was collected into 100 mL volumetric flask.

2 Preparation of $VO_2@SiO_2$ nanostructures

For synthesis of $VO_2@SiO_2$ nanostructures, reverse microemulsions were prepared by mixing 100.0 mL N-decane (97%, Aladdin) as a non-polar phase, 4.0 g cetyltrimethylammoniumbromide (CTAB, 99%, Aladdin) as a surfactant, 10.0 mL 1-hexanol (98%, Aladdin) as a cosurfactant, 5.0 mL V^{4+} solution prepared above as the polar phase. The compositions of our microemulsion mainly refer to Feldman's literature.[4]The microemulsion system was heated to 60°C under air atmosphere. After 30 min of magnetic stirring, a certain amount of 1 M ammonia ($NH_3 \cdot H_2O$, Sinopharm Chemical Reagent) was dropped to adjust the pH of microemulsion and the temperature was increased to 100°C within 10 min and maintained for 1-2 h. When the solution was cooled to near room temperature, 0.5 ml tetraethyl orthosilicate(TEOS,AR, Alladin) was added to above solution and stirred for another 2-4 h. Finally, 40 ml Diethylene glycol (DEG, CP, Sinopharm Chemical Reagent) was added in order to depress the reaction and to initiate a phase separation. The composites were collected from the DEG bottom phase by centrifugation. The solid was washed several times by redispersion in ethanol and centrifugation, and finally dried in an oven at 110°C for 2 h. The reaction conditions and resulting morphologies of precursors were listed in Table 1. In order to obtain well-crystallized VO_2 powder, heating treatment was required between 600 and 800°C for 1-3 h in N_2 atmosphere. The specific parameters of our experiment was listed in Table 1.

Table 1 Reaction conditions and reaction time for $VO_2@SiO_2$

Sample	TEOS(ml)	Heat-treatment time(min)
A1	0.3	10
A2	0.3	15
A3	0.3	20
B1	0.7	30
B2	0.7	45
C1	1.0	45
C2	1.0	90

Characterization

The crystal phases of the final products were conducted on a Rigaku Ultima IV X-ray diffractometer (XRD) with Cu Kα radiation (λ=1.5418Å). The morphology was characterized by transmission electron microscopy (TEM, JEM 4000EX, JEOL, Tokyo, Japan). The phase transition properties of the resulting products were measured by differential scanning calorimetry (DSC200F3, NETZSCH) with the temperature ranging from 0 to 100°C at a heating/cooling rate of 10°C/min, using a liquid nitrogen cooling unit. The thermochromic properties were evaluated by coating the powder onto float glass substrate. For measuring, the powders were coated on a slide of glass uniformly by a double-sided adhesive and highly transparent Teflon tape, which exhibits no thermochromic property. Transmittance and absorption curve of the sole tape-sticked glass was calibrated as baseline. The transmission (*Tr*) measurements was conducted at wavelength ranging from 250 nm to 2600 nm at 25°C and 100 °C on UV-Vis spectrophotometer (HITACHI U-3010) by inserting films in a temperature controlling unit.

For all samples, the integrated luminance transmittance(T_{lum}, 380-780nm), solar transmittance (T_{sol}, 240-2600nm) were obtained based on the measured spectra using the following equation:

$$T\rho = \int \psi_{\rho}(\lambda)T(\lambda)d\lambda / \int \psi_{\rho}(\lambda)$$

Where $T(\lambda)$ means the transmittance at wavelength λ, ρ denotes *lum*or *sol* for calculations, ψ_{lum} is the standard efficiency function for photopic vision, and ψ_{sol} is the solar irradiance spectrum for an air mass of 1.5 (corresponding to the sun standing 37^{o} above the horizon).

References

1 J. Livage, Materials, 2010, 3, 4175.
2 P. Souchay, Thermodynamique Chinique, 3rd. Masson, Paris(1968).
3 J. J. Legendre, J. Livage, J. Colloid Interface Sci. 1983, 94, 75.
4 R. Lopez, T. E. Haynes, L. A. Boatner, Optics. Lett., 2002, 27, 1327.
5 L. D. Landau, E. M. Lifshitz, Electrodynamics of Continuous Media [M] .Pergramon Press.,1984.
6 Hans, W; Verleur, A.S.; Barker, J.R.; Berglund, C.N. Phys. Rev. 1968, 172, 788